A test of common assumptions used to infer subglacial water flow through overdeepenings

Christine F. DOW,[1,2*] Jeffrey L. KAVANAUGH,[2] Johnny W. SANDERS,[3] Kurt M. CUFFEY[3,4]

[1]*Glaciology Group, College of Science, Swansea University, Swansea, UK*
E-mail: christine.f.dow@nasa.gov
[2]*Department of Earth and Atmospheric Sciences, University of Alberta, Edmonton, Alberta, Canada*
[3]*Department of Earth and Planetary Science, University of California, Berkeley, Berkeley, CA, USA*
[4]*Department of Geography, University of California, Berkeley, Berkeley, CA, USA*

ABSTRACT. Borehole instrument records from a cirque glacier with an overdeepened bed are examined to assess the validity of widely held glacial hydrological assumptions. At this glacier, hydraulic-potential calculations suggest water below overburden pressure will flow into the overdeepening, where the steepness of the riegel causes water to pool in the basin and increase in pressure. Our subglacial water pressure data also show high consistent pressures in the overdeepening and the presence of an active, variable-pressure drainage system towards the margin of the cirque. Therefore, we find that although uniform hydraulic-potential calculations are not directly applicable, they can still be useful for interpretation of the subglacial hydrological system. We also examine supercooling assumptions under different pressure and temperature regimes for water flowing over a riegel, driven using our borehole records of subglacial water temperatures that are consistently above the pressure-melting point during the late melt season. Our results show that even a slight increase in basal temperatures relative to the local pressure-melting point is sufficient to prevent a reduction in basal hydraulic conductivity as a result of supercooling freeze-on.

KEYWORDS: glacier flow, glacier hydrology, glacier modelling, mountain glaciers, subglacial processes

INTRODUCTION

The presence and flow of water at the bed of glaciers is widely known to affect ice motion (e.g. Iken and others, 1983; Shepherd and others, 2009), glacier stability (e.g. Kamb and others, 1985; Hulbe and Fahnestock, 2004) and basal erosion (e.g. Iverson, 1991; Cohen and others, 2006). Substantial difficulties exist, however, in directly examining the characteristics of subglacial hydrological systems, so a common alternative has been to use surface-based measurements to estimate basal water conditions. This requires the application of some simplifying assumptions. In particular, subglacial water flow paths are commonly estimated using calculations of hydraulic-potential gradients, following Shreve (1972), based on assumptions of uniform water pressure at the bed (e.g. Hagen and others, 2000; Pälli and others, 2003; Rippin and others, 2003; Ahlstrøm and others, 2005; Willis and others, 2009). For overdeepened regions of the glacier bed, supercooling calculations are often applied to assess whether water will freeze as it flows up the adverse bedrock slope (e.g. Alley and others, 1998; Lawson and others, 1998; Tweed and others, 2005; Cook and others, 2007; Cook and Swift, 2012).

In this paper, we use basal water pressure and temperature records from West Washmawapta Glacier, Canada, to assess how well standard assumptions regarding basal water pressure and temperature conditions apply to an overdeepened system. Our in situ data are compared with basal hydrological characteristics predicted from standard hydraulic-potential and supercooling equations.

*Present address: Cryospheric Sciences Lab, NASA Goddard Space Flight Center, Greenbelt, MD, USA.

THEORETICAL FRAMEWORK

Water flux, Q, at any point in a subglacial system can be defined as

$$\vec{Q} = -k\nabla\phi, \quad (1)$$

where k is the hydraulic conductivity of the subglacial system and $\nabla\phi$ is the gradient of hydraulic potential. Here we examine the impact of these two variables on basal water flux in relation to an overdeepened glacial system by examining (1) the topographic controls on water flow that directly affect $\nabla\phi$ and (2) the rate of supercooling-induced freezing on adverse slopes that affects k. First, following Shreve (1972), the equation for hydraulic potential, ϕ, in a subglacial system can be expressed as

$$\phi = \phi_0 + P_w + \rho_w g z_b = \phi_0 + f_w P_i + \rho_w g z_b, \quad (2)$$

where ϕ_0 is a reference potential, P_w is the water pressure, $\rho_w = 1000\,\mathrm{kg\,m^{-3}}$ is the density of water, $g = 9.81\,\mathrm{m\,s^{-2}}$ is the gravitational acceleration and z_b is the elevation of the bed. The $f_w = P_w/P_i$ term is a pressure coefficient in the form of a fraction of ice overburden ($P_i = \rho_i g(z_a - z_b)$, where z_a is the ice surface elevation and $\rho_i = 917\,\mathrm{kg\,m^{-3}}$ is the density of ice). Equation (1) can then be expressed as

$$\vec{Q} = -k(f_w\nabla P_i + P_i\nabla f_w + \rho_w g\nabla z_b), \quad (3)$$

and further expanded to

$$\vec{Q} = -k[P_i\nabla f_w + \rho_i g f_w(\nabla z_a - \nabla z_b) + \rho_w g\nabla z_b]. \quad (4)$$

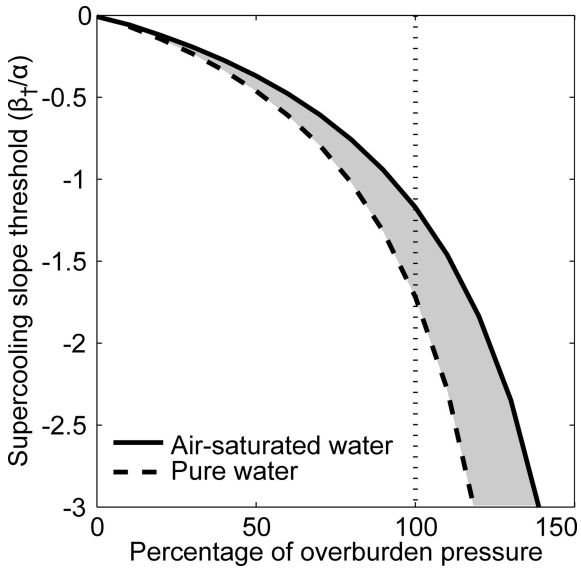

Fig. 1. Supercooling slope threshold as a function of basal water pressure, plotted as a percentage of overburden pressure (Eqn (8)).

Recognizing that basal water pressures have been observed to vary significantly over diurnal and seasonal timescales at many glaciers, several recent analyses of hydraulic potential (e.g. Hagen and others, 2000; Pälli and others, 2003; Rippin and others, 2003; Ahlstrøm and others, 2005; Willis and others, 2009; Banwell and others, 2013) have set $\nabla f_w = 0$, so that basal water pressure is a spatially uniform fraction of overburden and can be temporally varied between water flowing at atmospheric pressures with $f_w = 0$, and water flowing at ice overburden pressure with $f_w = 1$. In these analyses of subglacial water flow, Eqn (4) is further simplified by assuming $k = 1$, thereby giving

$$\vec{Q} = -\{f_w[\rho_i g(\nabla z_a - \nabla z_b)] + \rho_w g \nabla z_b\}. \quad (5)$$

For $f_w = 1$, Eqn (5) reduces to Shreve's (1972) expression for hydraulic-potential gradients. By assuming spatially uniform water pressure, Shreve (1972) estimated a limit of uphill flow of subglacial water using calculations of hydraulic potential. This adverse slope, β^*, is expressed as

$$\beta^* = -f_w\left(\frac{\rho_i}{\frac{\rho_w}{f_w} - \rho_i}\right)\alpha, \quad (6)$$

where α and β are the surface and bed slopes in the direction of maximum $\vec{Q}$. In the case where basal water pressures are everywhere at overburden (i.e. for $f_w = 1$), an adverse bed slope ~11 times the ice surface slope will effectively prohibit water flow; when $f_w < 1$, water flow is blocked at lower bed slope angles. However, it should be noted that such restrictions in flow up adverse slopes are applicable only where siphoning does not occur (e.g. by venting of basal passageways to the atmosphere by crevasses or moulins), as this would alter the total flow-path gradient of hydraulic potential.

Changes in the hydraulic conductivity, k, of the subglacial system can also affect flux of basal water. On an adverse slope, such as those found downstream of overdeepenings, k can decrease due to the freezing of supercooled water along flow paths. Basal water in an overdeepened region of a glacier will generally be at greater pressures, and thus at a lower melting point, than water in regions where ice is thinner. If basal waters in an overdeepened region are equilibrated with the local melting point, then flow of this water into regions of thinner ice results in 'supercooling' of the water with respect to the local melting point of the thinner-ice region. Supercooled water flowing sufficiently slowly equilibrates to the local temperature by forming frazil ice that nucleates onto suspended particles. This suspended ice then accretes to the glacier sole or the underlying substrate as anchor ice (e.g. Svensson and Omstedt, 1994; Hammar and Shen, 1995; Cook and others, 2006). Faster-flowing water will be warmed by viscous heating and will require greater cooling before frazil ice begins to form. The consequence of the supercooling phenomenon is that k decreases, reducing Q. If sufficient freezing occurs, k will approach zero and flux along the adverse slope ceases. The bed slope threshold, $\beta_\dagger$, above which k begins to decrease due to supercooling freeze-on is expressed by Alley and others (1998) for spatially uniform $f_w = 1$ as

$$\beta_\dagger = \frac{\rho_i \kappa}{\rho_i \kappa - \rho_w}\alpha. \quad (7)$$

Here $\kappa = 1 + \gamma C_s$ where $C_s = 4.2 \times 10^6\,\mathrm{J\,m^{-3}\,K^{-1}}$ is the volumetric specific heat of water; $\gamma = -9.8 \times 10^{-8}\,\mathrm{K\,Pa^{-1}}$ is the pressure dependence of the melting point for air-saturated water and $\gamma = -7.4 \times 10^{-8}\,\mathrm{K\,Pa^{-1}}$ for air-free water (the true value of γ is thus likely to fall between these two values). Freeze-on begins to occur at a minimum slope of $\beta_\dagger = -1.2\alpha$ for air-saturated water and $\beta_\dagger = -1.7\alpha$ for pure water, narrowing or blocking the flow path up the adverse slope (Röthlisberger and Lang, 1987; Alley and others, 1998).

Alley and others (1998) considered only the case in which basal water pressures are everywhere equal to the ice overburden pressure. To investigate the effects that different water pressures have on the freezing threshold, the pressure coefficient for spatially uniform pressure can be included in Eqn (7), giving

$$\beta_\dagger = -\frac{f_w(\rho_i \kappa)}{[\rho_w - f_w(\rho_i \kappa)]}\alpha. \quad (8)$$

The change in the freezing threshold as a function of f_w for both air-saturated and pure water is shown in Figure 1. With $f_w < 1$, the adverse basal slope necessary for supercooling freeze-on is shallower; with $f_w > 1$, water can flow up steeper adverse slopes without freezing. Basal water pressure therefore has a direct effect on the hydraulic conductivity of the subglacial system. As a result, glacial systems with strongly varying meltwater inputs (that in turn vary the basal pressure) might experience episodic freezing and thawing on adverse basal slopes within the subglacial drainage system. Such freeze/thaw cycles could occur both diurnally (Creyts and Clarke, 2010) and seasonally, depending on the configuration and evolution of the basal hydrological system.

The supercooling analysis of Alley and others (1998) included viscous dissipation of heat from the flow of water and the heat energy required to keep water at the melting point. However, their analysis did not consider that water residing in a subglacial aquifer could be warmed significantly by geothermal heating, possibly raising the temperature above the local melting point. If this warming occurs, the presence of a steep riegel might impact basal conductivity less than the above discussion suggests. Alley and

others (1998) calculate the heat flux, H_{MP} (W m^{-2}), necessary to maintain water at the melting point as

$$H_{MP} = Q_W \frac{\partial P_w}{\partial x} \gamma C_s, \quad (9)$$

where Q_W (m^3 s^{-1} m^{-1}) is the average water flux per unit glacier width and $\partial P_w/\partial x$ is the water pressure gradient. Neglecting heat lost to melting or conduction into ice, the total amount of heat energy (per unit glacier width per second) required to keep water at the melting point as it travels up the riegel can be determined by integrating in the x-direction along the basal flow path. This results in the replacement of the pressure gradient in Eqn (9) with the total elevation change, Δz, between the base and crest of the riegel so that $H_{MP} = Q_W \rho_w g \Delta z \gamma C_s$. Water flowing at a temperature T_w greater than the local melting point at the base of the riegel by $\Delta T = T_w - T_{mp}$ will carry with it thermal energy flux, $H_{\Delta T}$, which will counteract the tendency to freeze as it travels up-riegel. $H_{\Delta T}$ is related to the water flux by

$$H_{\Delta T} = Q_W \Delta T C_s. \quad (10)$$

Neglecting heat generated by viscous dissipation of the flowing water, the temperature above the local pressure-melting point at the base of the riegel necessary to offset supercooling is given by equating Eqns (9) and (10):

$$\Delta T = \gamma \rho_w g \Delta z. \quad (11)$$

For example, with a 100 m high riegel, an initial (air-saturated) water temperature of only ~0.1°C above the local pressure-melting point at the base of the riegel contains sufficient heat energy to prevent supercooling along the slope. If the water is flowing at a rate sufficient to generate significant viscous heating, then water even closer to the freezing point can exit over the riegel.

The equations described here suggest limits of subglacial flux in an overdeepened system based on both the potential gradient and the hydraulic conductivity of the system. We now use subglacial instrument observations from a cirque glacier with an overdeepened bed to examine the extent to which the limitations on water flow implied by the above hydraulic potential and supercooling freeze-on equations are applicable in situ.

SITE LOCATION AND METHODS

Subglacial hydrological data were collected during summer 2007 at West Washmawapta Glacier (WWG), a small cirque glacier on the eastern flank of Helmet Mountain, in the Vermilion Range of British Columbia, Canada, located at 51°10.6′ N, 116°20.0′ W. WWG has been the site of several investigations regarding ice dynamics and hydrology (Kavanaugh and others, 2010; Sanders and others, 2010, 2012; Dow and others, 2011). WWG is warm-based, has a surface area of ~1 km^2 and occupies a bowl-like overdeepening with a maximum ice thickness of ~185 m. A photogrammetry and ground-penetrating radar (GPR) survey by Sanders and others (2010) provided surface and basal digital elevation models (DEMs) of WWG, indicating that a riegel with a maximum adverse slope of 15° lies ~800 m downstream of the bergschrund. During 2007, ten boreholes were drilled to the base of WWG, four of which were instrumented with a combination of thermistors and pressure transducers (see Fig. 2 for instrument installation locations; the remainder of the boreholes were intended for repeat inclinometry). Three of the instrumented boreholes were drilled ~100 m apart along a line running from the margin of the glacier towards the deepest part of the overdeepening; this transect was located ~50 m up-glacier of the base of the riegel. Dow and others (2011) provide further information on instrument installation procedures.

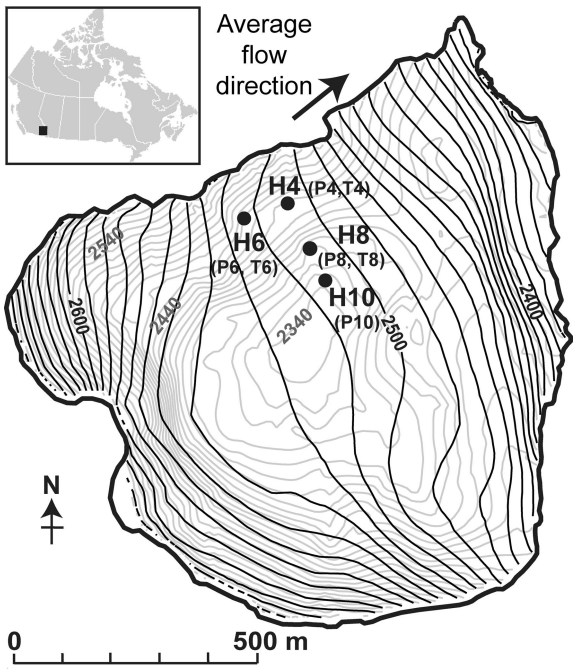

Fig. 2. Map of West Washmawapta Glacier showing locations of instrumented boreholes (circles) with their respective instruments (in parentheses). Bed and surface elevation contours are plotted in 10 m intervals in grey and black, respectively.

FIELD OBSERVATIONS AND INTERPRETATION

We present pressure transducer and thermistor data from sensors installed in boreholes H4, H6, H8 and H10 at WWG (Fig. 2). Instruments are named in reference to the borehole they occupy; for example, borehole H4 was instrumented with pressure sensor P4 and thermistor T4. Calibration procedures for the pressure transducers and the associated systematic errors are described by Dow and others (2011). Borehole H10 was blocked by a rock at 71 m depth; P10 was installed just above this obstruction. As a result, the depth of H10 could not be established through inclinometry or borehole observations. Instead, we estimated the ice thickness from GPR survey returns, which yielded a depth of 160 ± 10 m. P10 pressure values are therefore plotted relative to overburden, assuming an ice thickness of 160 m. As noted by Dow and others (2011), analysis of the borehole temperature data indicated that the long (~200 m) sensor wires used at WWG resulted in capacitance effects that offset the thermistor voltage/temperature relationship. Given this uncertainty, the data were calibrated by assuming that the greatest resistance value in each thermistor record represents a water temperature of −0.16°C; this value corresponds to the melting point at WWG's maximum measured ice thickness, plus an additional compensation of −0.04°C to account for the effect of impurities in the basal water (Harrison, 1975). This calibration method yields the lowest likely temperature values represented by the thermistor records, so the temperatures reported here are minimum estimates.

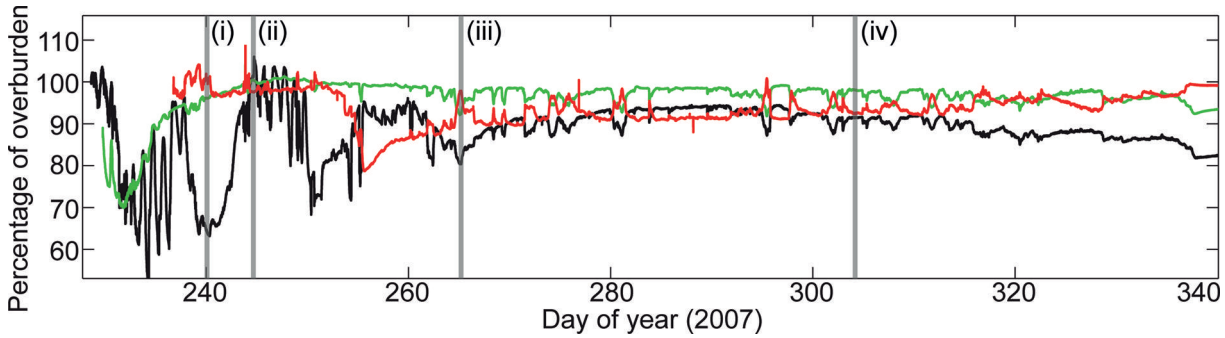

Fig. 3. Borehole pressure records plotted as a percentage of the overburden level: H4 (black curve), H8 (green curve) and H10 (red curve). The four vertical grey lines refer to the time periods shown in Figure 6.

The instrument records are discussed in detail by Dow and others (2011), who showed that basal water in the study region flows through a distributed, sediment-based subglacial drainage network. Water pressure values recorded in boreholes H4, H8 and H10 varied between ~50 and 105% of overburden over a range of timescales (Fig. 3), with peak pressures lagging daily maximum air temperatures by <2 hours. Water pressure fluctuations in the near-margin subglacial system (represented by borehole pressure records P4 and P8) altered the partitioning of overburden stress in the surrounding area, hydraulically jacking up the ice during times of increasing water pressures and thus lowering the overburden pressure (and hence water pressure) in the central portion of the glacier (represented by pressure record P10). As a result, there is a nearly perfect inversion of the pressure variations in H10 with respect to those recorded in H4 and H8 (Fig. 3).

Basal water temperatures in H4 and H6 varied on diurnal timescales and were generally inversely related to pressure in the corresponding borehole (Fig. 4). T8 temperature did not appear to diurnally fluctuate and there was little correlation between the T8 and P8 records. As a result, the T8 record is not shown or discussed further (Dow and others (2011) provide plots of the T8 record). As shown in Figure 4, the maximum diurnal temperature change in H4 was 0.80°C (day 255), while in H6 the maximum diurnal variation was 0.58°C (day 255). The maximum recorded water temperature in borehole H4 was ~0.75°C. However, it would be higher still if the record were calibrated relative to the local H4 melting point (−0.06°C) rather than the minimum glacier melting point (−0.16°C). High basal water temperatures are attributed to groundwater influx through a subglacial sediment aquifer. Dow and others (2011) hypothesize that at times of high pressure, cold meltwater was forced down into the sediment pack; conversely, at times of low subglacial water pressure, geothermally warmed groundwater could flow up through the sediment aquifer towards the ice/bed interface. It could be argued that temporal changes in solute concentration may be responsible for the observed temperature variations, with higher levels of dissolved sediment also allowing lower water temperatures than reported here. However, electrical conductivity measurements in H4 and H6 (Dow and others, 2011) indicate lower conductivity at times of lower water temperatures with diurnal variations on a scale of $<2\,\mu S\,cm^{-1}$ and an average conductivity of $\sim 51\,\mu S\,cm^{-1}$. This conductivity evidence suggests that dissolved sediment does not have a significant impact on basal water temperature at WWG.

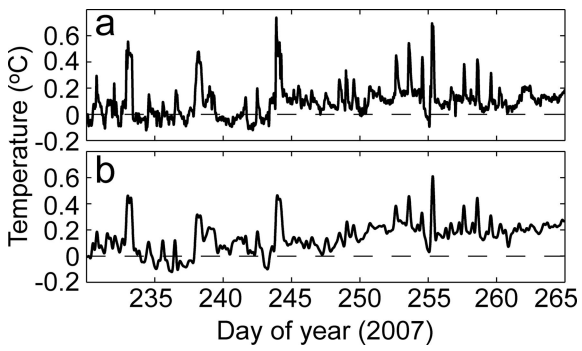

Fig. 4. Basal water temperature records from 18 August (day 230) to 22 September (day 265) 2007 recorded by (a) T4 and (b) T6, with the lowest temperatures referenced to the supercooling minimum (determined for the maximum ice thickness). The dashed line shows 0°C.

ANALYSIS

We now examine whether the controls on basal water flow suggested by hydraulic-potential and supercooling equations are observable in the WWG instrument records. In this section we discuss the following: (1) the applicability of a uniform pressure coefficient, f_w, to WWG, (2) the implications of the borehole pressure records for application of f_w, (3) whether the riegel slope is sufficiently steep to restrict water flow and (4) the implications of variable basal water temperatures on flow over the riegel. As noted above, a commonly used assumption is that water pressures under the glacier uniformly vary over time and space as a fraction of overburden (f_w; e.g. Arnold and others, 1998; Pälli and others, 2003; Ahlstrøm and others, 2005; Pattyn and others, 2005, 2009; Willis and others, 2009; Banwell and others, 2013). Using several uniform f_w values, we produce hydraulic-potential maps using surface and basal DEMs of WWG (Fig. 5). As noted by Sanders and others (2010), the depth/density profiles in the near-headwall regions of thick firn at WWG are poorly known. To assess the impact of this uncertainty on the hydraulic-potential gradient calculation, Schytt's (1958) relationship (also eqn (2.2) of Cuffey and Paterson, 2010, p. 19) was used to calculate a depth/density profile for firn in the regions of the glacier with surface elevations above the equilibrium-line altitude (ELA). This relationship is applied with values of $z_t = 50\,m$ and $z_p = z_t/1.9$ for the firn-to-ice transition and e-folding

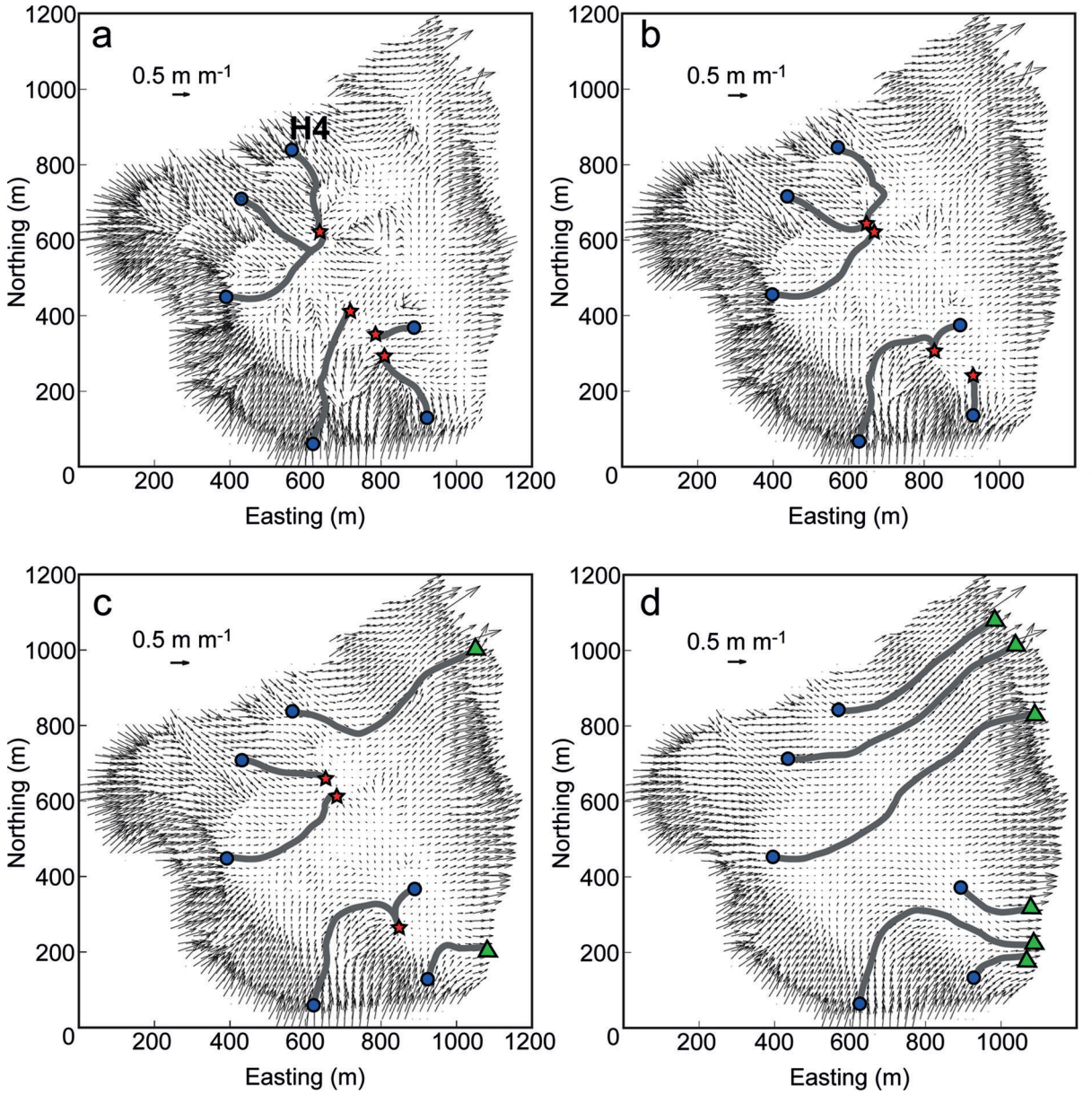

Fig. 5. Hydraulic-potential gradient maps for WWG. The calculated potentials are based on uniformly varied basal water pressures relative to ice overburden pressure. The scales (labelled 0.5 m m^{-1}) refer to the hydraulic potential change. (a) 50% of overburden, (b) 75% of overburden, (c) 85% of overburden and (d) 100% of overburden. The grey curves indicate the calculated water flow directions based on the hydraulic-potential gradients, determined at six fixed input points (shown by the blue circles). The red stars represent where water flow ceases due to potential convergence. The green triangles show where water exits at the glacier margin.

depths, respectively, an ELA of 2520 m and a minimum firn density of 400 kg m^{-3}. The ice-equivalent depth of the modelled firn layer was determined by integrating, at 0.1 m intervals, the firn density profile of Schytt (1955). It was assumed that the firn depth varied linearly with surface elevation between the ELA (where the firn depth is 0 m) and the glacier's highest surface elevation where the assumed firn depth is z_t, and that the density profile was truncated from the top down as elevation decreased. Using this method and the parameter values given above, the maximum ice-thickness correction is just over 8 m. Resulting hydraulic-potential gradients are slightly lower in magnitude (~15% at the most) in the region above the ELA when compared with the case where the glacier is assumed to have a density of 917 kg m^{-3} throughout; however, there is no difference in the indicated flow directions between the firn-and-ice and ice-only models.

Four hydraulic-potential maps using this density-adjusted method and $f_w = 0.5$, 0.75, 0.85 and 1.0 are shown in Figure 5. For each hydraulic-potential map, predicted water pathways from six fixed start positions are plotted, including a pathway from the location of borehole H4 (Fig. 5a). The hydraulic-potential gradients (and resulting water pathways) shown in Figure 5 suggest that, when pressures are 50–75% of overburden (Fig. 5a and b), water flows into the overdeepening and not over the riegel. At 85% of overburden (Fig. 5c) most of the water up-glacier of the riegel flows into the overdeepening; however, at the location of borehole H4, water can flow over the riegel and exit the glacier. Only when pressures approach overburden is water in the cirque driven predominantly down-glacier (Fig. 5d). The hydraulic-potential maps therefore indicate that water will tend to accumulate in the overdeepening until pressurized to a level near overburden. As a result, water in the overdeepening will

likely maintain pressures near overburden throughout the melt season, because water cannot escape over the riegel at lower pressures. This result, suggested by the uniform hydraulic-potential maps, is supported by the borehole pressure records. The basal water pressure in the near-margin borehole, H4, varies diurnally between 50% and 80% of overburden (e.g. day 234; Fig. 3), which suggests the presence of an active drainage system. However, boreholes located further within the overdeepening (H8 and H10) have pressures that are consistently close to overburden pressure, often with <10% of diurnal variation (Fig. 3).

We now further examine borehole pressure records on both diurnal and longer timescales. Boreholes H4, H8 and H10 form a 200 m long transect from near the margin towards the centre of the glacier. We use the borehole records to examine whether water pressures vary between the overdeepening and the near-margin region both diurnally and seasonally and, as a result, whether uniform applications of hydraulic-potential equations are directly applicable to WWG. In Figure 6 we plot the pressures for (1) four different days and (2) four times within a diurnal cycle (day 248). Figure 6a and b show the pressure plotted as a percentage of overburden. If water pressures were spatially uniform, they would appear as horizontal lines. Instead, the lines seesaw back and forth, indicating that there are substantial variations in basal water pressure from the margin towards the centre of the overdeepening. Water pressures in these boreholes tend to only approach a spatially uniform pattern at levels close to overburden. Figure 6c and d show the variation in the water table inferred from the borehole water levels across our transect. Assumptions that a water table should be approximately level across the glacier cross section have previously been applied to valley glaciers (Reynaud, 1973). This argument has been used to explain faster ice-sliding speeds in the centre of valley glaciers, where effective pressures will be lower than those found near the margins, in order to maintain a flat water table (Weertman, 1972). However, the water levels from the boreholes indicate that a flat water table at this cirque glacier is rarely achieved during the melt season. Instead, the water level (particularly near the margin) varies widely at WWG, similar to records seen at other valley glaciers (Fountain, 1994; Hubbard and others, 1995). Finally, Figure 6e and f show the basal hydraulic potential in the boreholes, calculated using the relative bed elevation as the z datum. Even with pressures near overburden, the relative hydraulic potential at borehole H10 is lower than near the margin. These plots also show that hydraulic potential for the three boreholes varies over time and not in spatial unison.

In order to determine whether the riegel at WWG is sufficiently steep to reduce the conductivity of the basal hydrological system by supercooling freeze-on, we compare the riegel slope with the thresholds predicted by Eqn (8), which can be used to predict what water pressures would be necessary to allow flow up the adverse slope. We calculate the basal and surface gradients on a grid of 10 m for the entire glacier, taking account of the direction of water flow suggested by the overburden hydraulic-potential calculations plotted in Figure 5d, to emulate downstream flow. The freezing threshold (i.e. $\beta_{\dagger}/\alpha$) is plotted in Figure 7a, assuming air-saturated water. The minimum pressure necessary for water to flow over the riegel without freezing due to supercooling equilibration is shown in Figure 7b. Figure 7 illustrates that the supercooling freeze-on conditions on the riegel vary substantially. Very little of the riegel has a gradient sufficiently shallow to allow supercooled water to flow over it without freezing, which suggests that the hydrological conductivity will decrease over time so that flux over the riegel is not possible. However, flow in proglacial streams throughout the melt season and diurnal changes in basal water pressure (specifically, the night-time drawdown of pressures) both demonstrate that water is exiting the glacial system. The only area of the riegel that does not require basal water pressures exceeding 150% of overburden to prevent supercooling freeze-on is directly downstream of the near-margin boreholes (Fig. 7).

Another factor influencing rates of supercooling freeze-on is the temperature of the water prior to flow up the riegel. If water temperatures are above the local melting point within the overdeepening, supercooling on the riegel is likely to be lessened, or possibly absent. Given that water temperatures at the base of WWG vary both diurnally and seasonally (Fig. 4), supercooling freeze-on might occur only during specific basal water flow conditions (e.g. times of high water pressure, when basal water temperatures are typically observed to be low). The maximum elevation difference between the deepest part of the overdeepening and the tip of the riegel is ~100 m. Equation (11) indicates that water would only need to be ~0.1°C above the melting point to prevent supercooling freeze-on over this change in elevation. The temperature record from H4 suggests that the only time that water temperatures dropped below this freezing threshold was between days 230 and 261 (18 August–18 September 2007), a period during which large diurnal variations in water pressures were observed in borehole H4 (~60–90% of overburden; Fig. 3). As shown in figure 7 of Dow and others (2011), water temperatures in this borehole remained high following the summer melt season and throughout the winter. However, early-melt-season temperature data were not recorded, so there may have been periods of lower water temperatures, allowing supercooling freeze-on earlier in the season. Despite this, from our available data, the only period during which supercooling freeze-on appears to have been likely at WWG occurred in the late summer melt season (days 230–261), when temperatures were close to the melting point and, for the most part, when basal water pressures were high.

DISCUSSION

Overdeepenings are common features underlying valley glaciers and ice sheets (Cook and Swift, 2012). By comparing hydraulic-potential and supercooling calculations with borehole records from an overdeepened glacier we raise questions particularly about analysis of drainage development for the many glaciers that flow through overdeepenings, although similar analyses could also be carried out at a glacier with a smoother basal topography. Most applications of hydraulic-potential theory implicitly assume that subglacial hydrological conditions (including hydraulic conductivity and water availability) are homogeneous. There is substantial evidence in the glaciological literature that this is not the case, particularly in reference to the Röthlisberger (1972) theory of subglacial channel formation (e.g. Hock and Hooke, 1993; Nienow and others, 1998; Bartholomew and others, 2011). At WWG, the strong hydraulic jacking signal (shown by the inverse response of P10 relative to the near-margin P4 and P8 records) indicates that the region of

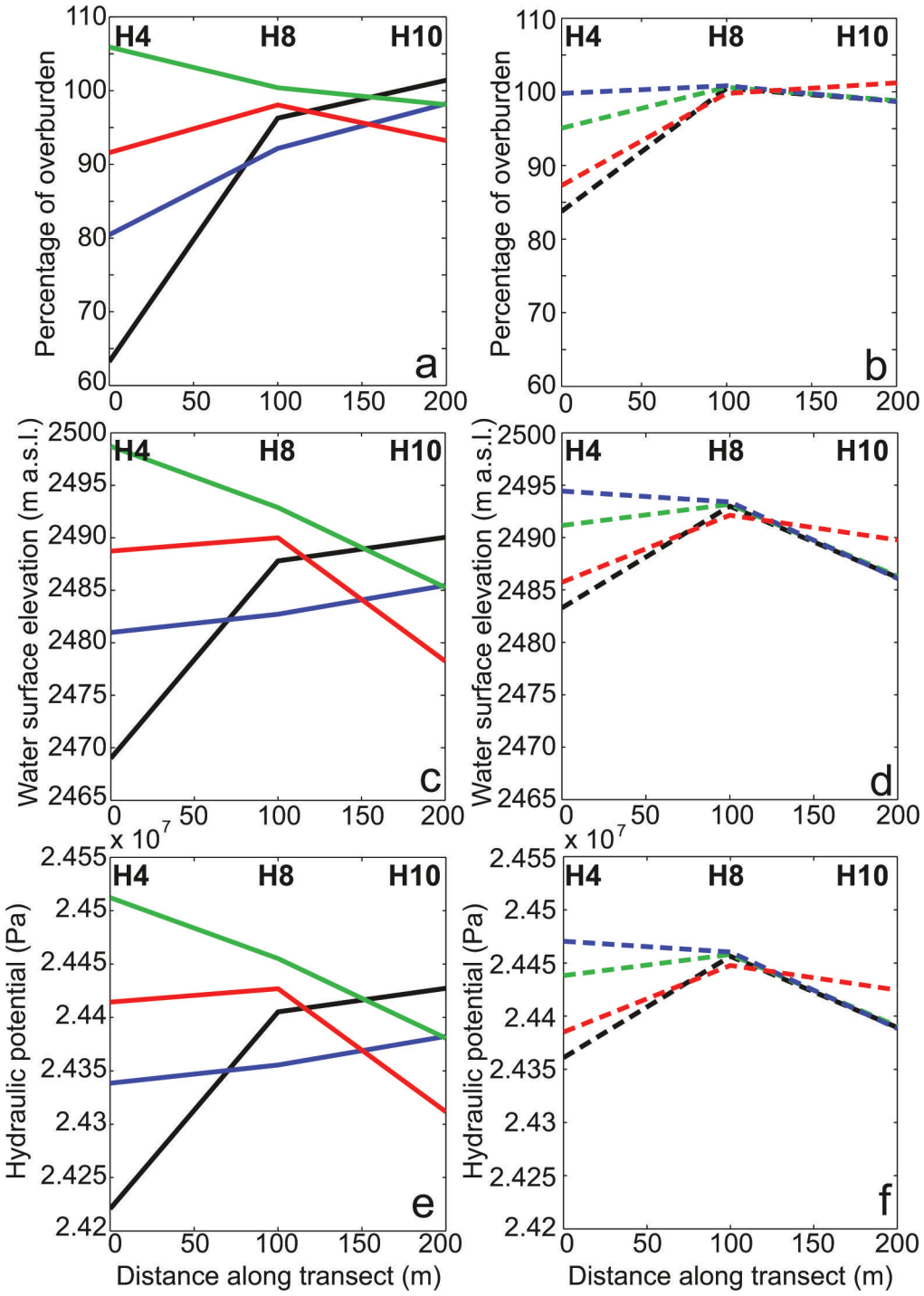

Fig. 6. Basal water pressures (expressed as (a, b) fraction of the local overburden pressure, (c, d) water surface elevation and (e, f) the basal hydraulic potential) along a transect from the margin towards the overdeepening using a linear interpolation of H4, H8 and H10 borehole pressure records. (a, c, e) Pressures are plotted as a percentage of overburden at the four time periods indicated in Figure 3: (i) solid black = 08:10 day 240, (ii) green = 17:30 day 244, (iii) blue = 02:30 day 265, (iv) red = 07:30 day 304. (b, d, f) Pressures plotted at four times during day 248 (5 September): dashed black = 06:00, dashed green = 12:00, dashed blue = 18:00, dashed red = 23:59.

the bed sampled by P10 is hydraulically isolated, demonstrating spatial variations in subglacial hydraulic conductivity or variable basal potential gradients directing water away from this region. Such factors demonstrate why hydraulic-potential calculations based on f_w and assuming homogeneous basal substrate could be misleading for estimating subglacial drainage characteristics.

At WWG the hydraulic-potential maps imply that water will pool in the overdeepening until pressures approach overburden. In addition, due to the steepness of the riegel in the overdeepening, water (particularly at lower pressures) is likely to encounter restricted (and perhaps blocked) flow paths due to supercooling freeze-on, further contributing to pooling of water in the overdeepening. As a result, the water pressure in the overdeepening can be expected to be consistently high. The borehole records support this interpretation of the hydraulic-potential maps, and indicate that water pressure is lower towards the margin of the glacier, whereas the water pressure near the overdeepening in the centre of the glacier is consistently closer to overburden pressure (Fig. 6).

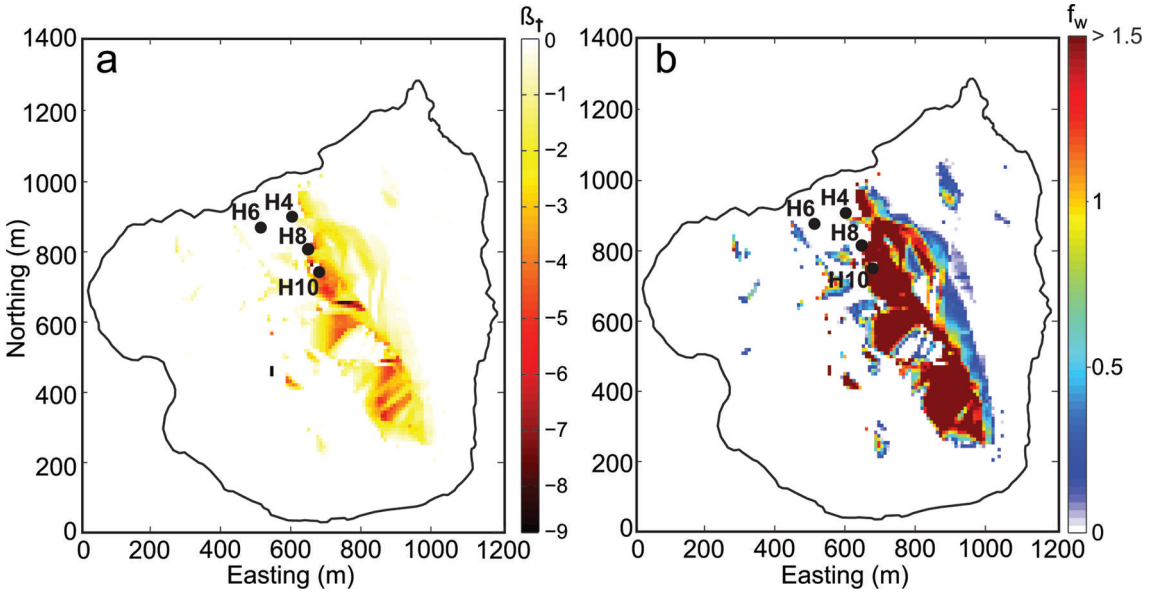

Fig. 7. Map of WWG showing (a) the gradient multiplier, $\beta_{\dagger}$, equivalent to the supercooling slope threshold shown in Figure 1 and (b) the minimum water pressure necessary for supercooled water to continue flowing at the bed of the glacier without freezing, expressed as a fraction of overburden, f_w. Borehole locations are indicated by black circles.

However, Figure 6a and b show that a uniform f_w does not capture the observed water pressure variations (which vary both spatially and temporally) at this cirque glacier. Despite this, as shown by the borehole records, the hydraulic-potential maps based on f_w can contribute to analysis of the basal hydrological system if interpreted with care.

Water flow near the cirque margin (as suggested by the borehole records) is also more likely than water flow into the overdeepening, as a result of the steepness of the riegel. As shown in Figure 7b, the only regions likely to allow water flux up the slope without significantly reducing the flow-path hydraulic conductivity are towards the margin of the cirque. Nonetheless, the strong fluctuations in subglacial water temperature, and above-freezing values recorded at WWG, suggest that supercooling freeze-on could occur over a much smaller fraction of the riegel downstream of the boreholes than is implied by Figure 7. If subglacial water temperatures exceed the local melting point throughout most of the glacier, it is possible that supercooling will occur over far less of the riegel's width than is suggested by the steepness of the basal slope. The high water temperatures measured near the riegel indicate that care should be taken when analysing other overdeepened systems that might be subject to supercooling, as the basal water might not be at the pressure-melting point up-glacier of the riegel. The combination of varying basal water temperature and pressure suggests the occurrence of supercooling in at least some glacial systems might be more spatially and temporally variable than is currently understood.

Sanders and others (2010) reported that very little basal motion occurs within the overdeepening, and that sliding is largely constrained to the near-margin areas of the cirque glacier and the riegel. Given that the hydraulic-potential calculations and borehole records suggest that water pressures in the overdeepening are consistently high and stable (which should encourage ice flow) compared with diurnally varying water pressures near the margin, this suggests that ice flux in the overdeepening is restricted by something other than water availability. Instead, the presence of the adverse slope is likely to be an important control on ice velocity (Cook and Swift, 2012). The current hydrological and dynamic configuration of this glacier has implications for the erosional history of the cirque, as the current structure is not suitable for further development of the overdeepening. There is perhaps a self-regulating threshold (similar to that suggested by Alley and others, 2003), where the adverse slope is steepened by erosion until water flux becomes highly restricted from supercooling freeze-on, although with geothermal heating of water as our data suggest, this threshold may be steeper than that proposed by Alley and others (2003). With limited water flux in the overdeepening, the basal drainage system might reorganize, driven by higher pressures in the centre of the cirque basin, so water flow is primarily near the glacier margin, as suggested by the borehole pressure records.

CONCLUSIONS

We have tested assumptions behind topographic hydraulic-potential and supercooling controls on water flow, using instrument records from a cirque glacier with an overdeepened bed. At this glacier during the summer months, spatially variable water pressures suggest that calculations of uniform hydraulic potential at overburden pressure are unlikely to be directly applicable. Outputs from hydraulic-potential equations using uniform pressures below overburden suggest that water will flow into the overdeepening. Because at this lower pressure water cannot exit over the riegel, it will pool and pressure will build up. Our borehole records along a cross-flow transect support this, showing water pressures close to overburden towards the middle of the cirque and variable pressures (both diurnally and on longer timescales) near the cirque glacier margin. Both the hydraulic-potential maps and the borehole records can therefore be interpreted as representing a mostly inactive hydrological system in the overdeepening and an active hydrological system towards the glacier margin. However, although uniform hydraulic-potential calculations are not

directly applicable to the basal drainage system of this glacier, the hydraulic-potential maps can be used to assess subglacial hydrological conditions if interpreted with care.

The steepness of the riegel, combined with a lower pressure-melting point within the overdeepening, suggests that water should freeze on the riegel at most pressures observed at this glacier. However, we have records of water temperatures above the pressure-melting point for much of the late summer and winter season, which indicate that supercooling will only occur at specific times of day during the summer melt season. If high basal temperatures occur at other glaciers with overdeepenings, supercooling may also be limited under these bodies of ice. Our results illustrate the necessity for further study of supercooling in overdeepened systems.

ACKNOWLEDGEMENTS

This research was funded by the National Science and Engineering Research Council of Canada, the US National Science Foundation (grant No. NSF GLD-0518608 to K.M.C.), the Canadian Circumpolar Institute and the University of Alberta. C.F.D. was funded by the Alberta Ingenuity Fund and a UK Natural Environment Research Council doctoral scholarship. We thank the British Columbia Ministry of Agriculture and Lands for permission to conduct fieldwork in the study area, and J. Beckers for assistance in the field.

REFERENCES

Ahlstrøm AP, Mohr JJ, Reeh N, Christensen EL and Hooke RLeB (2005) Controls on the basal water pressure in subglacial channels near the margin of the Greenland ice sheet. *J. Glaciol.*, **51**(174), 443–450 (doi: 10.3189/172756505781829214)

Alley RB, Lawson DE, Evenson EB, Strasser JC and Larson GJ (1998) Glaciohydraulic supercooling: a freeze-on mechanism to create stratified, debris-rich basal ice: II. Theory. *J. Glaciol.*, **44**(148), 563–569

Alley RB, Lawson DE, Larson GJ, Evenson EB and Baker GS (2003) Stabilizing feedbacks in glacier-bed erosion. *Nature*, **424**(6950), 758–760 (doi: 10.1038/nature01839)

Arnold N, Richards K, Willis I and Sharp M (1998) Initial results from a distributed, physically-based model of glacier hydrology. *Hydrol. Process.*, **12**(2), 191–219 (doi: 10.1002/(SICI)1099-1085(199802)12:2<191::AID-HYP571>3.0.CO;2-C)

Banwell AF, Willis IC and Arnold NS (2013) Modeling subglacial water routing at Paakitsoq, W Greenland. *J. Geophys. Res.*, **118**(3), 1282–1295 (doi: 10.1002/jgrf.20093)

Bartholomew I and 6 others (2011) Supraglacial forcing of subglacial drainage in the ablation zone of the Greenland ice sheet. *Geophys. Res. Lett.*, **38**(8), L08502 (doi: 10.1029/2011GL047063)

Cohen D, Hooyer TS, Iverson NR, Thomason JF and Jackson M (2006) Role of transient water pressure in quarrying: a subglacial experiment using acoustic emissions. *J. Geophys. Res.*, **111**(F3), F03006 (doi: 10.1029/2005JF000439)

Cook SJ and Swift DA (2012) Subglacial basins: their origin and importance in glacial systems and landscapes. *Earth-Sci. Rev.*, **115**(4), 332–372 (doi: 10.1016/j.earscirev.2012.09.009)

Cook SJ, Waller RI and Knight PG (2006) Glaciohydraulic supercooling: the process and its significance. *Progr. Phys. Geogr.*, **30**(5), 577–588 (doi: 10.1177/0309133306071141)

Cook SJ, Knight PG, Waller RI, Robinson ZP and Adam WG (2007) The geography of basal ice and its relationship to glaciohydraulic supercooling: Svínafellsjökull, southeast Iceland. *Quat. Sci. Rev.*, **26**(19–21), 2309–2315 (doi: 10.1016/j.quascirev.2007.07.010)

Creyts TT and Clarke GKC (2010) Hydraulics of subglacial supercooling: theory and simulations for clear water flows. *J. Geophys. Res.*, **115**(F3), F03021 (doi: 10.1029/2009JF001417)

Cuffey KM and Paterson WSB (2010) *The physics of glaciers*, 4th edn. Butterworth-Heinemann, Oxford

Dow CF, Kavanaugh JL, Sanders JW, Cuffey KM and MacGregor KR (2011) Subsurface hydrology of an overdeepened cirque glacier. *J. Glaciol.*, **57**(206), 1067–1078 (doi: 10.3189/002214311798843412)

Fountain AG (1994) Borehole water-level variations and implications for the subglacial hydraulics of South Cascade Glacier, Washington State, USA. *J. Glaciol.*, **40**(135), 293–304

Hagen JO, Etzelmüller B and Nuttall A-M (2000) Runoff and drainage pattern derived from digital elevation models, Finsterwalderbreen, Svalbard. *Ann. Glaciol.*, **31**, 147–152 (doi: 10.3189/172756400781819879)

Hammar L and Shen HT (1995) Frazil evolution in channels. *J. Hydraul. Res.*, **33**(3), 291–306 (doi: 10.1080/00221689509498572)

Harrison WD (1975) Temperature measurements in a temperate glacier. *J. Glaciol.*, **14**(70), 23–30

Hock R and Hooke RLeB (1993) Evolution of the internal drainage system in the lower part of the ablation area of Storglaciären, Sweden. *Geol. Soc. Am. Bull.*, **105**(4), 537–546 (doi: 10.1130/0016-7606(1993)105<0537:EOTIDS>2.3.CO;2)

Hubbard BP, Sharp MJ, Willis IC, Nielsen MK and Smart CC (1995) Borehole water-level variations and the structure of the subglacial hydrological system of Haut Glacier d'Arolla, Valais, Switzerland. *J. Glaciol.*, **41**(139), 572–583

Hulbe CL and Fahnestock MA (2004) West Antarctic ice-stream discharge variability: mechanism, controls and pattern of grounding-line retreat. *J. Glaciol.*, **50**(171), 471–484 (doi: 10.3189/172756504781829738)

Iken A, Röthlisberger H, Flotron A and Haeberli W (1983) The uplift of Unteraargletscher at the beginning of the melt season – a consequence of water storage at the bed? *J. Glaciol.*, **29**(101), 28–47

Iverson NR (1991) Potential effects of subglacial water-pressure fluctuations on quarrying. *J. Glaciol.*, **37**(125), 27–36

Kamb B and 7 others (1985) Glacier surge mechanism: 1982–1983 surge of Variegated Glacier, Alaska. *Science*, **227**(4686), 469–479 (doi: 10.1126/science.227.4686.469)

Kavanaugh JL, Moore PL, Dow CF and Sanders JW (2010) Using pressure pulse seismology to examine basal criticality and the influence of sticky spots on glacial flow. *J. Geophys. Res.*, **115**(F4), F04025 (doi: 10.1029/2010JF001666)

Lawson DE, Strasser JC, Evenson EB, Alley RB, Larson GJ and Arcone SA (1998) Glaciohydraulic supercooling: a freeze-on mechanism to create stratified, debris-rich basal ice. I. Field evidence. *J. Glaciol.*, **44**(148), 547–562

Nienow PW, Sharp M and Willis IC (1998) Velocity–discharge relationships derived from dye tracer experiments in glacial meltwaters: implications for subglacial flow conditions. In Sharp MJ, Richards KS and Tranter M eds. *Glacier hydrology and hydrochemistry*. Wiley, Chichester, 103–118

Pälli A, Moore JC, Jania J, Kolondra L and Glowacki P (2003) The drainage pattern of Hansbreen and Werenskioldbreen, two polythermal glaciers in Svalbard. *Polar Res.*, **22**(2), 355–371 (doi: 10.1111/j.1751-8369.2003.tb00117.x)

Pattyn F, de Brabander S and Huyghe A (2005) Basal and thermal control mechanisms of the Ragnhild glaciers, East Antarctica. *Ann. Glaciol.*, **40**, 225–231 (doi: 10.3189/172756405781813672)

Pattyn F, Delcourt C, Samyn D, De Smedt B and Nolan M (2009) Bed properties and hydrological conditions underneath McCall Glacier, Alaska, USA. *Ann. Glaciol.*, **50**(51), 80–84 (doi: 10.3189/172756409789097559)

Reynaud L (1973) Flow of a valley glacier with a solid friction law. *J. Glaciol.*, **12**(65), 251–258

Rippin D and 6 others (2003) Changes in geometry and subglacial drainage of Midre Lovénbreen, Svalbard, determined from digital elevation models. *Earth Surf. Process. Landf.*, **28**(3), 273–298 (doi: 10.1002/esp.485)

Röthlisberger H (1972) Water pressure in intra- and subglacial channels. *J. Glaciol.*, **11**(62), 177–203

Röthlisberger H and Lang H (1987) Glacial hydrology. In Gurnell AM and Clark MJ eds. *Glacio-fluvial sediment transfer: an alpine perspective*. Wiley, Chichester, 207–284

Sanders JW, Cuffey KM, MacGregor KR, Kavanaugh JL and Dow CF (2010) Dynamics of an alpine cirque glacier. *Am. J. Sci.*, **310**(8), 753–773 (doi: 10.2475/08.2010.03)

Sanders JW, Cuffey KM, Moore JR, MacGregor KR and Kavanaugh JL (2012) Periglacial weathering and headwall erosion in cirque glacier bergschrunds. *Geology*, **40**(9), 779–782 (doi: 10.1130/G33330.1)

Schytt V (1955) Glaciological investigations in the Thule ramp area. *SIPRE Rep.* 28

Schytt V (1958) Glaciology II(C). The inner structure of the ice shelf at Maudheim as shown by core drilling. In *Norwegian–British–Swedish Antarctic Expedition, 1949–52, scientific results*. Norsk Polarinstitutt, Oslo, 113–151

Shepherd A, Hubbard A, Nienow P, McMillan M and Joughin I (2009) Greenland ice sheet motion coupled with daily melting in late summer. *Geophys. Res. Lett.*, **36**(1), L01501 (doi: 10.1029/2008GL035758)

Shreve RL (1972) Movement of water in glaciers. *J. Glaciol.*, **11**(62), 205–214

Svensson U and Omstedt A (1994) Simulation of supercooling and size distribution in frazil ice dynamics. *Cold Reg. Sci. Technol.*, **22**(3), 221–233 (doi: 10.1016/0165-232X(94)90001-9)

Tweed FS, Roberts MJ and Russell AJ (2005) Hydrologic monitoring of supercooled meltwater from Icelandic glaciers. *Quat. Sci. Rev.*, **24**(22), 2308–2318 (doi: 10.1016/j.quascirev.2004.11.020)

Weertman J (1972) General theory of water flow at the base of a glacier or ice sheet. *Rev. Geophys.*, **10**(1), 287–333 (doi: 10.1029/RG010i001p00287)

Willis I, Lawson W, Owens I, Jacobel R and Autridge J (2009) Subglacial drainage system structure and morphology of Brewster Glacier, New Zealand. *Hydrol. Process.*, **23**(3), 384–396 (doi: 10.1002/hyp.7146)

MS received 3 February 2014 and accepted in revised form 20 June 2014